Article
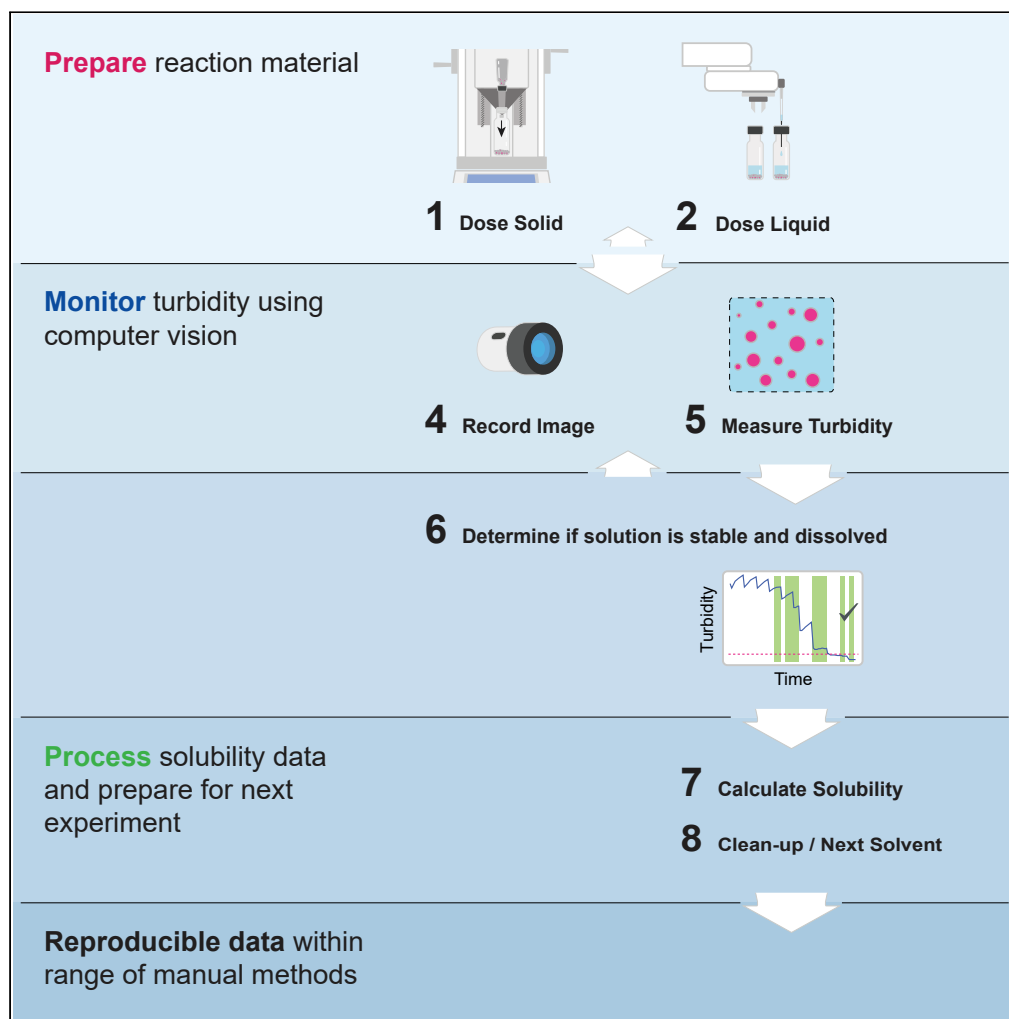
Automated solubility screening platform using computer vision

Parisa Shiri,
Veronica Lai, Tara
Zepel, ..., Fan
Yang, Paloma L.
Prieto, Jason E.
Hein

jhein@chem.ubc.ca

HIGHLIGHTS

We demonstrate a
modular, closed-loop
robotic platform for
solubility screening

Automated solvent
titration is informed by
computer vision and
turbidity monitoring

No human intervention or
HPLC analysis is required
during the experimental
loop

Solubility values obtained
by the system match those
obtained via traditional
methods

Article

Automated solubility screening platform using computer vision

Parisa Shiri,[1] Veronica Lai,[1] Tara Zepel,[1] Daniel Griffin,[2] Jonathan Reifman,[2] Sean Clark,[1] Shad Grunert,[1] Lars P.E. Yunker,[1] Sebastian Steiner,[1] Henry Situ,[1] Fan Yang,[1] Paloma L. Prieto,[1] and Jason E. Hein[1,3,*]

SUMMARY

Solubility screening is an essential, routine process that is often labor intensive. Robotic platforms have been developed to automate some aspects of the manual labor involved. However, many of the existing systems rely on traditional analytic techniques such as high-performance liquid chromatography, which require pre-calibration for each compound and can be resource consuming. In addition, automation is not typically end-to-end, requiring user intervention to move vials, establish analytical methods for each compound and interpret the raw data. We developed a closed-loop, flexible robotic system with integrated solid and liquid dosing capabilities that relies on computer vision and iterative feedback to successfully measure caffeine solubility in multiple solvents. After initial researcher input (<2 min), the system ran autonomously, screening five different solvent systems (20-80 min each). The resulting solubility values matched those obtained using traditional manual techniques.

INTRODUCTION

Solubility is defined as the amount of a compound that will dissolve in a certain amount of solvent at a given temperature when the system is in equilibrium. The ability to reliably screen solubility is fundamental to many areas of chemical research and industry sectors, from pharmaceutical applications (Coltescu et al., 2020; Hansen, 1969), where solubility is used for process development and solvent selection, to material science, where it limits formulation and processing parameters (Hansen, 2004; Machui et al., 2012; Walker et al., 2011). Common methods to determine solubility, which can be broadly categorized as 'excess solid' or 'excess solvent' methods, typically require researchers to perform incremental, manual tasks such as solid dosing that must be adjusted and repeated for each solute-solvent system (Black et al., 2013). In the case of excess solid, solute is added to a solution until excess undissolved solids are observed in the sample. The solution is allowed to equilibrate for a long incubation time and is then sampled and analyzed for composition using a variety of analytic techniques (e.g., gravimetric methods, titration, UV-spectrometry, or most commonly high-performance liquid chromatography or HPLC). The excess solid method with filtration, also called 'shake-plate' or 'slurry', is known to provide the highest quality data. However, it requires the additional step of filtration or at-temperature centrifugation prior to analysis (Selekman et al., 2017), which adds experimental complexity and slows down the workflow (Hoelke et al., 2009).

In the excess solvent method, a titration-like procedure is applied: solvent is added stepwise to a solute until a fully dissolved state is observed. The composition of the solution and the dissolution point are then typically measured using light scattering or imaging-based technology (Reus et al., 2015). The excess solvent method can therefore obviate the need for pre-calibrated and expensive analytical methods like HPLC, but it comes at the cost of adding the somewhat time-consuming stepwise solvent addition actions.

Recent advances in technology have enabled the development of automated robotic platforms (Burger et al., 2020; Li et al., 2018; MacLeod et al., 2020) that aid in decreasing hands-on experimental time and increasing throughput (Selekman et al., 2017). While effective when applied to solubility screening (Goodwin, 2006; Selekman et al., 2017; Sou and Bergström, 2018), most existing systems are only partially automated and still require human intervention and interpretation at many stages of the workflow. In addition, these systems continue to rely on analytical techniques that require time-consuming method development as well as calibration prior to the solubility screen.

[1]Department of Chemistry, University of British Columbia, Vancouver, BC V6T 1Z1, Canada

[2]Amgen Inc., Cambridge, MA 02141, USA

[3]Lead contact

*Correspondence: jhein@chem.ubc.ca

https://doi.org/10.1016/j.isci.2021.102176

The vast majority of automated solubility screening systems rely on HPLC, the most common analytical instrument applied in excess solid strategies (Alsenz et al., 2007; Chen et al., 2002; Qiu et al., 2020; Tan et al., 2005; Wenlock et al., 2011). While reliable and a standard method for quantifying the amount of material in a solution, HPLC has several drawbacks – the most significant in the context of automation is that it requires calibration. Moreover, a UV chromophore must be present on each set of test materials and researcher time is spent developing the customized methods necessary for accurate analysis.

Other automated platforms have used *in situ* techniques for analysis. For example, Dinter et al. (Dinter et al., 2005) have reported a solubility screening platform using a fiberoptic turbidity probe for qualitative solubility measurements, categorizing the solution as soluble, turbid or uncertain within a range. Other groups have reported using a UV plate reader for solubility measurements in both absorption and light scattering modes (Chen et al., 2002; Hoelke et al., 2009). Dehring et al. (Dehring et al., 2004) developed a system that uses stepwise addition of solvent and laser-based nephelometry for high-throughput measurement of aqueous solubility. However, a human researcher is still required for solid dosing and visual checks. Machine vision offers a minimally invasive and direct means of assessment and has been extensively used in a wide range of applications in chemistry such as thin film defect detection (Taherimakhsousi et al., 2020), lab object recognition (Eppel et al., 2020), as well as solubility studies. Stukelj et al. (Štukelj et al, 2019a, 2019b, 2020) have reported an image-based single-particle-analysis method to measure amorphous solubility. Reus et al. have used vision to determine clear points based on images taken by a ReactIR probe. While less time-consuming and hands-on than HPLC, such methods still require calibration and the addition of a probe or controlled emission of light, which may not be accurate due to limited detection (Reus et al., 2015).

Here we present a modular, closed-loop robotic platform for automating solubility screening by combining a titration (excess solvent) method with simple computer vision. Unlike the majority of solubility screening platforms which make use of HPLC as the analytical method, this system is HPLC-free, relying solely on images recorded by the webcam and a custom algorithm to monitor turbidity and determine when the solid material in a solution is dissolved. The platform's design is purposefully modular, enabling its easy adaptation to other workflows such as crystallization and multi-solvent systems. In addition, the system can be accessed via remote desktop and a security camera, which easily allows the user to have a live view of the experiment or perform further development on the system remotely (see Table S1 and Figure S7 in the Supplemental information (SI) document, for further details).
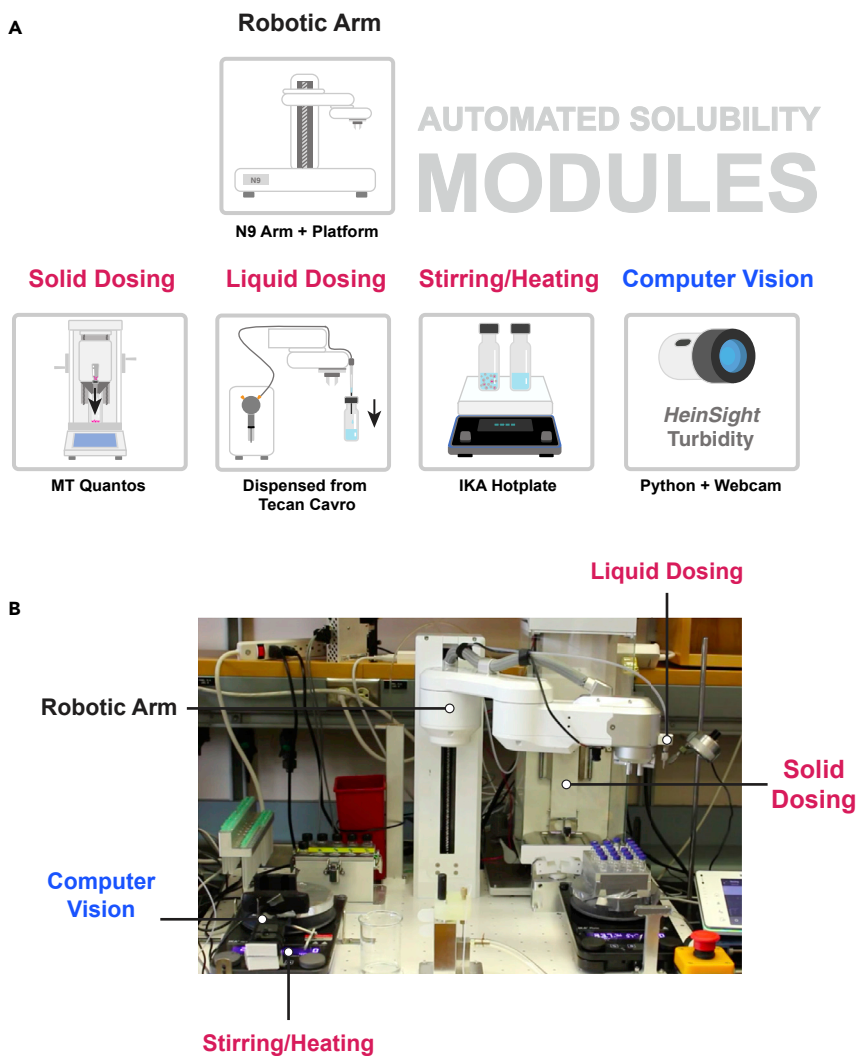
RESULTS

Automation platform modules

Our automated platform consists of five basic modules: (1) a robotic arm, (2) liquid dosing system, (3) solid dosing unit, (4) stir plate, and (5) webcam (Figure 1A). Each module performs an essential component of solubility testing: (1) manipulating objects, (2) dosing solvents, (3) adding solid, (4) controlling reaction conditions, and (5) recording images for turbidity study, respectively. All modules were connected to the lab computer. While fully integrated and run from a Python master script, the modules are designed to function independently, thereby enabling easy reconfiguration or expansion to suit a given set of experimental conditions. All modules are located atop a robotic deck (Figure 1B) equipped with additional hardware components and general-purpose tools that help the modules interact (see Figure S1 for further detail).

N9 robotic arm

The N9 is a Selective Compliance Articulated Robot Arm (SCARA) equipped with a rotatable gripper and a probe (North Robotics, www.northrobotics.com). It consists of 3 elbows and can move in three dimensions. Both gripper and probe are attached to the arm head and used to handle specific equipment needed for the solubility workflow. The N9 gripper is used to transfer, uncap, and recap HPLC vials, while the probe is used to handle needles for liquid dosing. Additional hardware components are placed on the N9 deck and can be engaged by the arm to run experiments.

Liquid dosing

The liquid dosing module consists of a Tecan Cavro syringe pump connected to the N9 controller. One port is connected to a solvent reservoir and the other to the N9 probe, enabling sampling to and from any vial on the deck. The solvent reservoir can contain any solvent, acetonitrile in our case, and was used to prime the

A

Robotic Arm

AUTOMATED SOLUBILITY
MODULES

N9 Arm + Platform

Solid Dosing	Liquid Dosing	Stirring/Heating	Computer Vision
MT Quantos	Dispensed from Tecan Cavro	IKA Hotplate	*HeinSight* Turbidity — Python + Webcam

B

Liquid Dosing

Robotic Arm

Solid Dosing

Computer Vision

Stirring/Heating

Figure 1. Automated solubility screening modules (N9 platform)
(A) Modules on the platform including the specific equipment used.
(B) A front view of module positioning on the robotic deck.

tubing line prior to any liquid dosing. The syringe for the pump can hold 1 mL and accurately deliver between 0.01 mL to 0.95 mL. Solvents are located on the deck in vials capped by pre-slit septa to minimize solvent evaporation and contamination while allowing sampling with a needle on the end of the N9 probe. Refer to Figures S1 and 1B.

Solid dispensing

In a solubility screening workflow, it is important to be able to accurately dose a specified amount of solid. An on-deck solid dosing system extends the capabilities of an automated solubility screening platform. However, most existing platforms continue to rely on manual solid dosing and are therefore only partially automated (Alsenz et al., 2007). In this platform, we make use of a Mettler Toledo Quantos powder dosing system with custom modifications to integrate solid dispensing into the automated workflow. After initial filling of the dosing heads with the desired compound, all solid dosing is completed without human intervention. The Quantos is additionally used as a balance. The direct measurement of mass of all materials dispensed (both solid and liquid) is then used to gravimetrically calculate solubility. For further detail on the custom-built parts used with the Quantos, refer to Figures S2–S4.
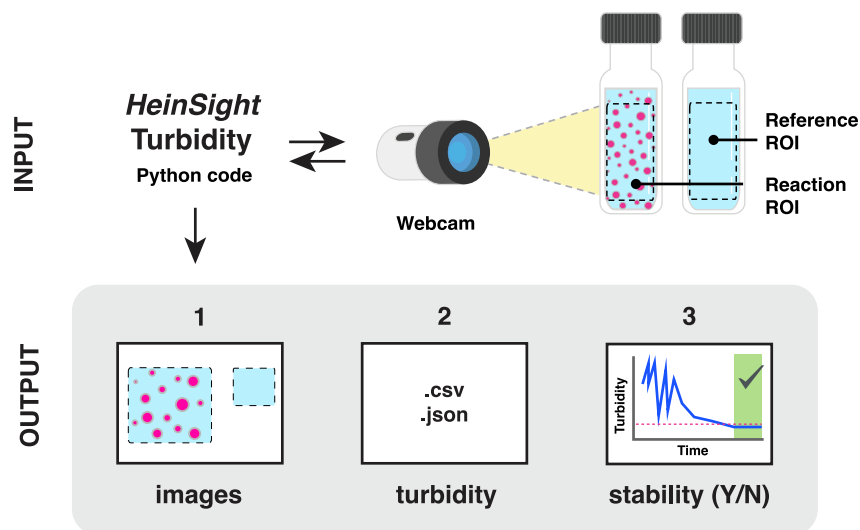
Figure 2. Overview of HeinSight component of the computer vision module

The HeinSight turbidity code reads in images captured by a webcam and analyzes the pixels within a preselected region of interest to arrive at a proxy turbidity value. Recorded images, turbidity data, and graphs of turbidity over time are saved as the output. In the turbidity graph, the reference lines are graphed as a dashed red line, and when stability is found, the background area is shaded green.

Stirring

An IKA RCT digital stir plate is used to stir vials containing solvent and solute mixtures. To prevent the vials from moving on the plate as they are stirred, vials are placed in a vial holder called the "vision station". The holder is designed with an open front to enable visual monitoring of the vial contents while placed inside (refer to Figure S6 for further details).

Computer vision

The computer vision component of the platform relies on HeinSight, an open-source Python package previously developed by our group to automate common laboratory tasks usually based on visual observation (Zepel et al., 2020). It is responsible for a key component in our automated workflow: monitoring and measuring turbidity. The turbidity module, specifically designed for the purpose of solubility screening, analyzes the turbidity of a solution from recorded images without the need to build a reference library or additional calibration. Images captured by a basic webcam are processed using a custom algorithm that measures the average brightness of a given solute/solvent combination. Because turbidity is an optical property characterized by how the suspended and dispersed solids scatter light (Lawler, 2013), and most organic systems are composed of a clear solvent and a near-white solid, average brightness serves as a proxy for relative turbidity in most situations. The value output by our algorithm is then referenced against an image of pure solvent and a decision is made as to whether the solution is fully dissolved or not (Figure 2).

The decision to use a simple computer vision method in this case limits the workflow's application to solute/solvent systems that meet the expectations of relatively clear solvent and bright solid. While more sophisticated computer vision methods for measuring turbidity exist (Liu et al., 2018), they typically rely on a standard comparison library that must be hand-built, requiring significant investment in time on the part of a human researcher as well as specialized laboratory equipment. Using a far simpler method in this case allowed us to demonstrate the validity of the automated solubility workflow using the simplest variant of the computer vision module.

Automated workflow

The modules are integrated in a closed-loop workflow that is designed to mimic how a human researcher would manually conduct experiments. The automated solubility screen workflow described here was run
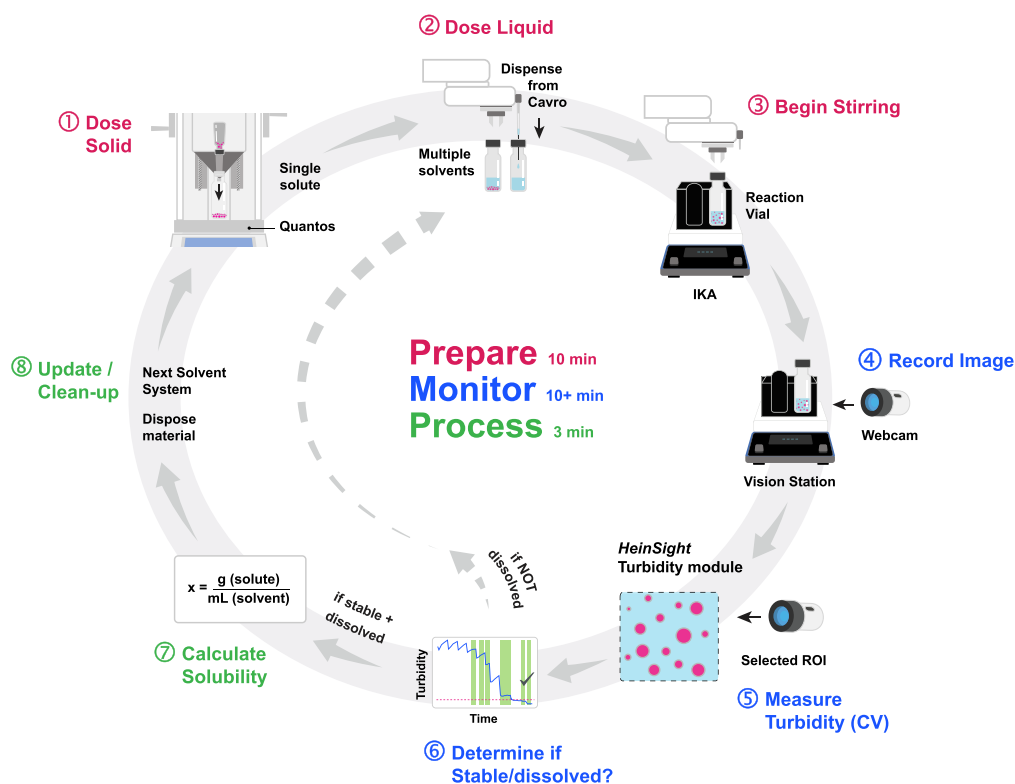
Figure 3. Automated workflow overview

(1) A fresh HPLC vial is uncapped and transferred to the Quantos where a pre-specified amount of solid is dispensed. The vial is then recapped and transferred to the vision station. (2) A pre-specified initial volume of solvent is dispensed into the vial with the solid and stir bar. The system starts stirring in (3). In (4), (5), and (6), turbidity monitoring takes place. In (7) the solubility is calculated based on solid mass and final solvent volume. In (8), the used vial is returned to the tray and the system updates initial values in preparation for the next experiment.

via a master Python script with each module being controlled using custom code packages. The workflow can be broken down into three stages: prepare, monitor, and process (Figure 3). In the preparation stage, the researcher sets the experiment parameters and the region of interest (ROI) to monitor turbidity for the rest of the workflow. After this initial input, the N9 arm prepares a vial with the solid to dissolve and an initial volume of solvent and places it in the vision station. During the monitoring stage, the arm periodically adds a set volume of solvent into the vials while the computer vision module visually monitors turbidity until it determines the solution is fully dissolved or the maximum safe volume in the vial has been reached. Finally, in the processing stage, the vial with dissolved solution is weighed and properly disposed of, data are processed to determine the solubility of the solute and solvent combination, and experimental parameters are automatically selected for the next solute/solvent combination.

Initial system setup is minimal. The researcher should make sure the solid, solvents, and clean vials charged with stir bars are available on the deck as well as provide the input values for initial parameters such as initial amount of solid and solvent and stir rate. See the user documentation section of the Supplemental information for further detail. Once started, the system will follow the programmed workflow, automatically updating values and iterating through experiments until the solubility screen of each solid and solvent combination is complete or an interruption due to error or a pause request occurs. A detailed description of each step involved in the automated workflow follows.

Robotic methods

The script is run, and immediately a reference vial of pure solvent is prepared: the arm brings an empty vial to the vision station and adds the initial amount of solvent. The researcher is prompted to select a region in the

image to normalize all turbidity measurements and the region to monitor turbidity. The average brightness of all pixels in the region monitored is taken as the dissolved reference.

Step 1: solid dose

The arm takes a clean vial from the tray to the deck gripping station and uncaps the vial. The cap is temporarily parked on the pillar (refer to Figure S5). The arm then transfers the vial to Quantos. Once the vial is placed inside the Quantos, the balance tares and starts dosing. After dosing the Quantos z stage drives upwards, allowing the arm to enter the Quantos chamber and bring the vial back to the gripping station for recapping. Recapping uses torque feedback from the arm to tighten the cap by a single degree until the torque associated with a properly tightened cap is reached. For details on Quantos accessories and uncapping and recapping refer to the Supplemental information.

Step 2: initial solvent dose

The arm transfers the vial to the vision station and doses the initial volume of solvent into the vial. The syringe pump enables liquids to be drawn and dispensed precisely when there is a needle on the end of the probe. The arm can pick up a capped needle from the needle tray and uncap it using an uncapping tooth. To ensure needle handling is done properly, a smart vision feedback system is implemented (refer to Figure S8). In order to eliminate air bubbles in the line used to draw liquids, the line must first be primed by a backing solvent. Prior to drawing solvent into the lines for dosing a 50 μL air gap is drawn, part of which is injected into the solvent bottle the solvent is stored in to compensate for the volume to be drawn. The remaining air is kept to create distance between the drawn solvent and back solvent used to prime the line. After drawing in liquid, a second air gap is drawn to prevent solvent from dripping out of the needle during arm movements until the solvent is dispensed.

Step 3: computer vision screening and step addition of solvent

While solution turbidity in the vial is monitored, the needle remains on the arm probe and is used to dose fixed volumes of solvent as directed by the computer vision module. These additions of solvent comprise the step addition of solvent used to fully dissolve the solid in the vial with volumes ranging from 10 to 30 μL.

Step 4: transferring back vial and report generation

Once the computer vision module identifies that the solid has fully dissolved in the vial or if the safe volume of the vial is reached, the arm then discards the needle and takes the vial to the Quantos to weigh the vial. As the mass of just the vial and solid was previously measured, the mass and thus volume of solvent in the vial can be calculated directly. With the mass of solid and solvent known solubility can be gravimetrically determined. This also means that discrepancies between the volume that the script commanded the pump to dispense and the actual volumes dispensed are accounted for when calculating solubility. All the data gathered from the experiment is stored in real time. In addition, key data such as solubility status, solid and solvent types, amounts and errors are sent through Slack as real-time updates (refer to Supplemental information for more details). The slack report update provides a monitoring tool for the user which is especially valuable during the workflow development process.

Step 5: determining the next experiment

For the next experiment, the experiment parameters are discussed in the closed-loop control logic section of the Supplemental information. The duration of this step varies depending on when the dissolved state or the safe solvent volume in the vial is reached.

Computer vision methods

The HeinSight turbidity module is fully integrated into the automated workflow and includes the computer algorithm that determines control decisions based on visual input. Figure 4 shows how the steps involved in turbidity monitoring fit within the larger automated workflow.

Step 1: Select the ROI

First, the robot fills a vial with pure solvent, which is transferred to the vision station and measured to obtain the dissolved reference value. The user is then prompted to select two ROI. The first ROI, the normalization ROI, is used to normalize brightness for the turbidity value measurement as described in step 2 below
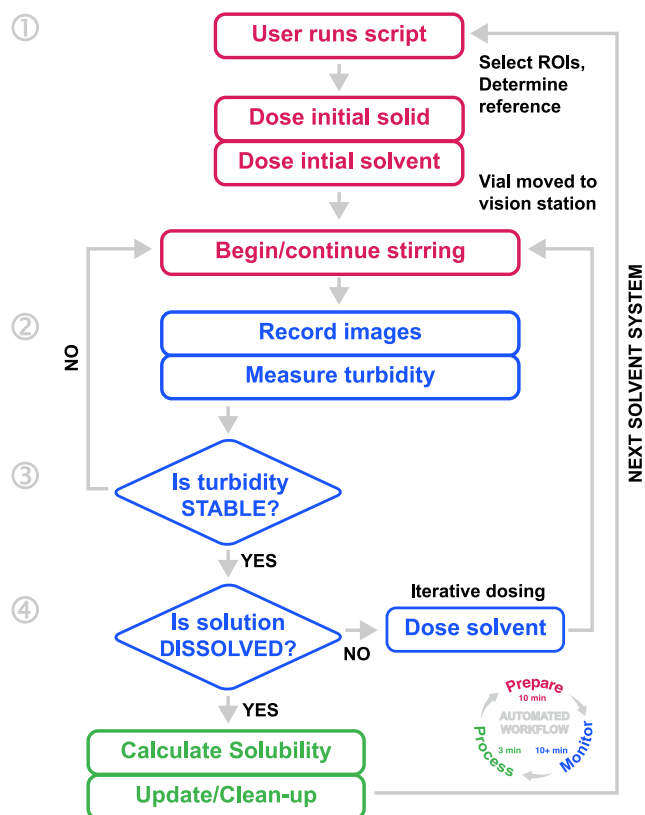
Figure 4. Expanded workflow showing control decisions and detailed steps of turbidity monitoring

(Figure 5). The second ROI defines the area within which the algorithm will monitor turbidity and capture the dissolved reference.

Step 2: Capture image and measure turbidity

Images are captured by the webcam and analyzed using a custom turbidity algorithm that proceeds in two steps: (1) pre-process and (2) calculate average brightness in the preselected ROI. To combat issues that may arise due to environmental changes in lighting, the average brightness in the ROI is normalized using a stable region in the image. While turbidity values for each image are recorded, the value used to determine stability (step 3) is an average across multiple consecutive images. This further reduces noise that may arise due to lighting changes or artifacts in the image.

Step 3: Determine if stable

An algorithm checks for trends in turbidity values over time and determines if the solution is stable based on statistical features (mean, median, mode, standard deviation, and range) of the most recent turbidity measurements. If the solution is determined to be stable and has not yet reached the dissolved reference or maximum volume, more solvent is added and monitoring continues.

Step 4: Determine if dissolved

If the solution is determined to be stable, the control algorithm checks for a fully dissolved state by comparing the current turbidity value to the dissolved reference. If "dissolved," the algorithm triggers a stir burst to agitate any solute that may have settled at the bottom of the vial. Once turbidity has stabilized at the reference value or if the five most recent minutes of turbidity data are all below the reference value then the solution is classified as dissolved. Details of the stir burst and statistical requirements for determining stable and dissolved states can be found in the Supplemental information.
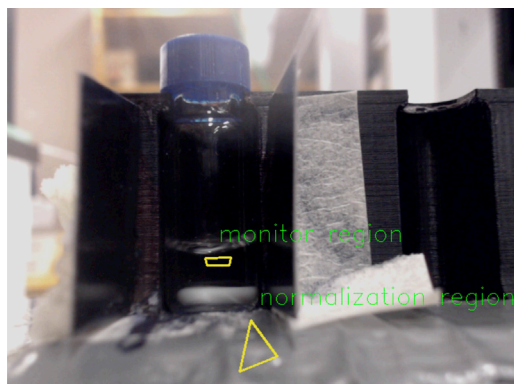
Figure 5. Example of an image taken by the camera with ROIs overlaid

Yellow outlines show the region where turbidity is being monitored in the reaction vessel (upper polygon) and region used for brightness normalization (lower triangle).

Workflow application: caffeine solubility

To illustrate the applicability of this workflow, we used the N9 automated platform to determine the solubility of caffeine in a variety of common organic solvents (acetonitrile, water, acetone, ethanol, and methanol). The experiments were tested with various initial solid values to challenge the control algorithm.
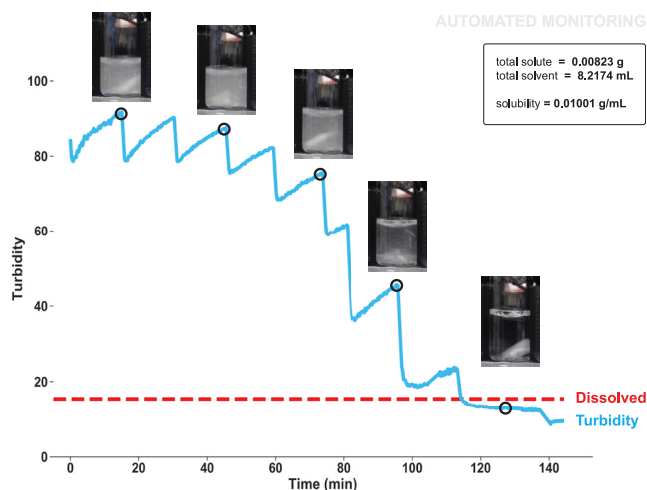
Figure 6 shows the turbidity of caffeine in acetone over time. The sharp decreases in turbidity correspond to points when additional solvent was added because the solution was determined to be stable. The stepwise behavior in this experiment can be explained by the incremental addition of solvent. Following each addition, large particles are further broken down by stirring, which visually manifests as increased turbidity. This trend was observed for some solvents at certain initial volumes; different solvents and different initial volumes produced different trend lines. The control algorithm is programmed to trigger a short stir-burst as turbidity nears the dissolved reference to ensure there is no solid left undissolved. The final step around 100 min can be explained by this increase in rate. Once the turbidity value reaches a stable point near or consistently below the dissolved reference, monitoring ceases and the workflow continues to the processing portion of the workflow. Occasionally, the turbidity value will read below the dissolved reference due to fluctuations in lighting (for more information, see Figure S9).

The control algorithm includes additional checks that account for similar experimental complexities. For example, once the turbidity value is within a specified range from that of the dissolved reference, the stir rate is increased for five minutes to ensure full dissolution of the solid. Turbidity monitoring continues and the algorithm then re-checks that a dissolved state has truly been reached. The platform ran for almost 2 days without error or interruption, allowing us to obtain precise and reproducible solubility values within range of those obtained via manual methods without the usual demands on human labor and with far greater speed.

Table 1 compares the mean solubility values obtained by our automated platform across four repeat experiments to those obtained via manual methods of slurry filtration (HPLC analysis) and titration. By comparison, data collection for the slurry method took approximately one week excluding calibration and method development while the titration method took three weeks due to the need for active researcher presence. For more information on the manual methods, refer to Manual Data Collection Process in the Supplemental information; for complete N9 solubility data, see Table S2.

Duplication: Kinova arm and TBZ solubility

To further showcase the modularity and broad applicability of the developed workflow, we replaced the N9 (SCARA) with a 6-axis robotic arm. The Kinova Gen3 arm has seven degrees of freedom and is equipped with a Robotiq 2F-85 gripper. Figure 7 shows the system setup with the new arm installed. Because the Kinova Gen3 is supported by a Python package, we were able to apply the master script previously used by N9 to run the solubility workflow to the new arm with minimal adaptation. Required changes included different arm movements as well as a different liquid handling system. The new liquid handling system has a few advantages: larger solvent reservoirs are attached to the line without the need to restock often compared to the on-deck solvent bank previously used on the N9 deck. Needle handling is also avoided with this system by using a sampler (For further details on this liquid handling system refer

Figure 6. Turbidity of caffeine in acetone over time

Annotated graph overlaid with images. Real-time turbidity values are shown in blue; the dotted red line indicates the dissolved reference measured by the system (turbidity of pure solvent).

to Figures S10 and S11). The sampler could be picked up by the gripper on the arm and sample or inject. Moreover, a vial holder was used as a regripping station to switch between horizontal and vertical gripping as needed. For reference, video demonstrations of the overall workflow on the N9 (Video S1) and the Kinova (Video S2) are included in the Supplemental information.

Table 2 compares the average solubility of triplicate measurements obtained by the two platforms, N9 and Kinova. In order to demonstrate reproducibility and show the capacity of either system to screen a more complex solute, we ran solubility experiments on tetrabenazine or TBZ (a yellowish powder) in acetone, ethanol, acetonitrile and methanol. As can be seen, the platforms yielded similar values across all solute/solvent combinations. Initial difference between observed values for some systems was attributed to the tendency of solid particles to cling to the inside of the vial walls when not properly cleaned, thereby skewing the turbidity value and affecting final gravimetric calculation. For more information, see the Computer vision challenges for turbidity section of the Supplemental information.

DISCUSSION

Here we report on a modular automated solubility screening platform that uses our HeinSight computer vision system and a feedback algorithm to implement a titration 'excess-solvent' workflow. As proof of concept, we used the platform to find the solubility of caffeine in various clear solvents; however, the system could be used to screen the solubility of any solid/solvent system with minimal modification. The purposefully modular design allows for easy adaptation and expansion to other robotic platforms or solubility study workflows as illustrated by the duplication using another robotic arm. For the next iteration of the platform, we developed a method to automate the exchange of the dosing head on the Quantos, thereby enabling the solubility screen to investigate multiple solute systems within a single workflow. The

Table 1. Comparison of solubility values obtained by manual and automated methods

Solvent	Slurry (mg/ml)	Titration 1 (mg/ml)	Titration 2 (mg/ml)	N9 avg. (mg/ml) $\pm$ SEM
Acetonitrile	20.6	17.6	18.4	19.18 $\pm$ 0.811
Water	20.2	17	18.5	18.21 $\pm$ 0.404
Acetone	10.7	8.7	7	9.98 $\pm$ 0.017
Ethanol	5.0	5	4.5	5.37 $\pm$ 0.059
Methanol	9.0	8.9	6.6	8.36 $\pm$ 0.81

SEM = standard error of mean.
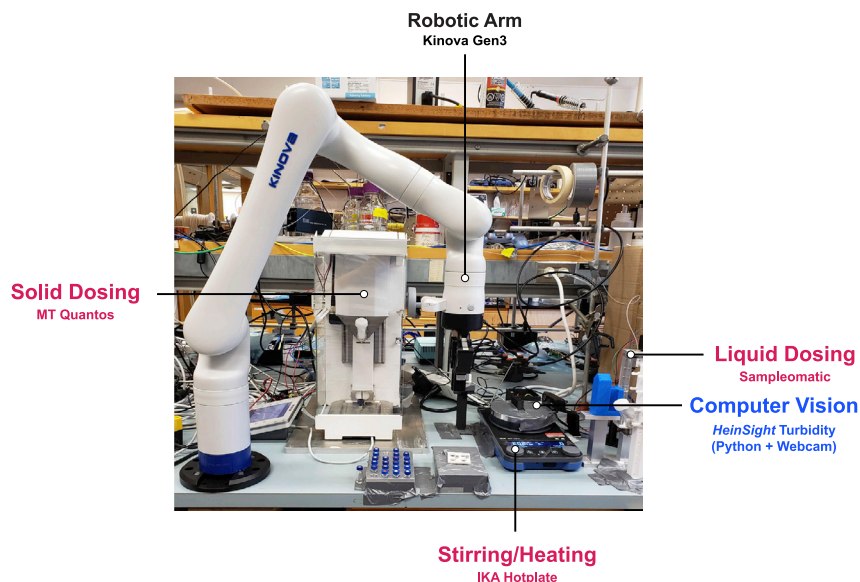
Figure 7. Automated solubility screening modules (Kinova platform)

workflow could likewise be expanded for use in automated crystallization and binary solvent analysis. We have additionally begun work on implementing a machine-learning based computer vision approach trained on the images collected during this study, which will allow for more accurate turbidity measurement and be able mitigate variation due to solid clumping or environmental changes in lighting. In summary, the modular robotic platform we developed demonstrates the benefits of flexible automation and was successfully used to perform automated solubility screens. We expect that the platform can facilitate finding answers to solubility questions in industries dealing with novel materials. By automating a process that is integral to experimental design and optimization, we hope to reduce demands on both material cost and human time.

Limitations of the study

The reported platform and workflow meet the base-case needs for automating solubility screening using computer vision. Using brightness as a proxy for turbidity offers a minimally invasive way of measuring relative turbidity with minimal computational processing. However, this approach requires a primarily white or white-like solute and clear solvent, which is true of most common solute/solvent systems. Minimal changes can be made to the code to accommodate other systems with more unusual coloring. Moreover, the computer vision algorithm can be challenged by significant changes to the visual environment. For example, strong fluctuations in light or glare on the vial will affect the accuracy of the turbidity measurement. See the Ambient Light Study section of the Supplemental information for further discussion. Developing a more robust computer vision module is essential to pushing the platform behind its current instantiation. It is also worth noting that the platform, as reported, does not focus on high throughput but rather the

Table 2. Solubility values obtained by N9 and Kinova platforms

Solute	Solvent	N9 avg. (mg/ml) $\pm$ SEM	Kinova avg. (mg/ml) $\pm$ SEM
Caffeine	Acetonitrile	19.18 $\pm$ 0.811	22.15 $\pm$ 0.827
Caffeine	Ethanol	5.37 $\pm$ 0.059	4.17 $\pm$ 0.279
TBZ	Acetone	88.12 $\pm$ 0.237	87.97 $\pm$ 0.882
TBZ	Ethanol	16.29 $\pm$ 0.237	16.18 $\pm$ 0.793
TBZ	Acetonitrile	67.81 $\pm$ 1.088	67.92 $\pm$ 5.48
TBZ	Methanol	25.03 $\pm$ 0.291	24.51 $\pm$ 0.206

automated gathering of reliable solubility data end-to-end with no human intervention. Throughput could easily be increased with the addition of parallel testing.

Resource availability

Lead contact
Further information and requests for resources should be directed to and will be fulfilled by the lead contact, Jason Hein (jhein@chem.ubc.ca).

Materials availability
This study did not generate new materials.

Data and code availability
All code used for this study is available at: https://gitlab.com/heingroup/automated_solubility_h1.

Further details regarding the custom-built packages as well as the data collected can be found in the Supplemental information. Additional information is available upon request.

METHODS

All methods can be found in the accompanying Transparent methods supplemental file.

SUPPLEMENTAL INFORMATION

Supplemental information can be found online at https://doi.org/10.1016/j.isci.2021.102176.

ACKNOWLEDGMENTS

AUTHOR CONTRIBUTIONS

J. E. H. and D. G. conceived the project. J. E. H. supervised the project. P. S. and S. G. developed the robotic workflow. V. L. and T. Z. developed the machine vision. P. S. and V. L. developed the master script and P. S., V. L., and S. G. designed and performed the experiments. J. R. collected the non-robotic solubility data. L. P. E. Y., H. S., S. S., S. C., and V. L. developed the software packages. S. S. and H. S. developed the robotic hardware. P. S. and F. Y. developed the robotic workflow on the Kinova platform. All authors participated in manuscript writing.

DECLARATION OF INTERESTS

The authors declare no competing interests.

REFERENCES

Alsenz, J., Meister, E.v. a., and Haenel, E. (2007). Development of a partially automated solubility screening (PASS) assay for early drug development. J. Pharm. Sci. *96*, 1748–1762.

Black, S., Dang, L., Liu, C., and Wei, H. (2013). On the measurement of solubility. Org. Process. Res. Dev. *17*, 486–492.

Burger, B., Maffettone, P.M., Gusev, V.V., Aitchison, C.M., Bai, Y., Wang, X., Li, X., Alston, B.M., Li, B., Clowes, R., et al. (2020). A mobile robotic chemist. Nature (London) *583*, 237–241.

Chen, T., Shen, H., and Zhu, C. (2002). Evaluation of a method for high throughput solubility determination using a multi-wavelength UV plate reader. Comb. Chem. High Throughput Screen. *5*, 575–581.

Coltescu, A.-R., Butnariu, M., and Sarac, I. (2020). The importance of solubility for new drug Molecules. Biomed. Pharmacol. J. *13*, 577–583.

Dehring, K.A., Workman, H.L., Miller, K.D., Mandagere, A., and Poole, S.K. (2004). Automated robotic liquid handling/laser-based nephelometry system for high throughput measurement of kinetic aqueous solubility. J. Pharm. Biomed. Anal. *36*, 447–456.

Dinter, C., Schuetz, A., Blume, T., Weinmann, H., Harre, M., and Neh, H. (2005). Automated solubility determination using a customized robotic system and a turbidity probe. J. Lab. Automation *10*, 408–411.

Eppel, S., Xu, H., Bismuth, M., and Aspuru-Guzik, A. (2020). Computer vision for recognition of materials and vessels in chemistry lab settings and the vector-LabPics data set. ACS Cent. Sci. *6*, 1743–1752.

Goodwin, J.J. (2006). Rationale and benefit of using high throughput solubility screens in drug discovery. Drug Discov. Today. Tech. *3*, 67–71.

Hansen, C.M. (2004). 50 Years with solubility parameters—past and future. Prog. Org. Coat. *51*, 77–84.

Hansen, C.M. (1969). The universality of the solubility parameter. Product R&D *8*, 2–11.

Hoelke, B., Gieringer, S., Arlt, M., and Saal, C. (2009). Comparison of nephelometric, UV-spectroscopic, and HPLC methods for high-throughput determination of aqueous drug solubility in Microtiter plates. Anal. Chem. (Washington) *81*, 3165–3172.

Lawler, D.M. (2013). Turbidity, Turbidimetry, and Nephelometry. Reference Module in Chemistry (Molecular Sciences and Chemical Engineering).

Li, J., Lu, Y., Xu, Y., Liu, C., Tu, Y., Ye, S., Liu, H., Xie, Y., Qian, H., and Zhu, X. (2018). AIR-chem: Authentic intelligent robotics for chemistry. J. Phys. Chem. *122*, 9142–9148.

Liu, Y., Chen, Y., and Fang, X. (2018). A review of turbidity detection based on computer vision. IEEE Access *6*, 60586–60604.

Machui, F., Langner, S., Zhu, X., Abbott, S., and Brabec, C.J. (2012). Determination of the P3HT:PCBM solubility parameters via a binary solvent gradient method: impact of solubility on the photovoltaic performance. Solar Energ. Mater. solar Cell *100*, 138–146.

MacLeod, B.P., Parlane, F.G.L., Morrissey, T.D., Häse, F., Roch, L.M., Dettelbach, K.E., Moreira, R., Yunker, L.P.E., Rooney, M.B., Deeth, J.R., et al. (2020). Self-driving laboratory for accelerated discovery of thin-film materials. Sci. Adv. *6*, eaaz8867.

Qiu, J., Patel, A., and Stevens, J.M. (2020). High-throughput screening of synthetic intermediates: effects of solvents, counterions, and counterion solubility. Org. process Res. Dev. *24*, 1262–1270.

Reus, M.A., van der Heijden, A.E.D.M., and ter Horst, J.H. (2015). Solubility determination from clear points upon solvent addition. Org. process Res. Dev. *19*, 1004–1011.

Selekman, J.A., Qiu, J., Tran, K., Stevens, J., Rosso, V., Simmons, E., Xiao, Y., and Janey, J. (2017). High-throughput automation in chemical process development. Annu. Rev. Chem. Biomol. Eng. *8*, 525–547.

Sou, T., and Bergström, C.A.S. (2018). Automated assays for thermodynamic (equilibrium) solubility determination. Drug Discov. Today. Tech. *27*, 11–19.

Štukelj, J., Agopov, M., Yliruusi, J., Strachan, C.J., and Svanbäck, S. (2020). Machine-vision-enabled salt dissolution analysis. Anal. Chem. *92*, 9730–9738.

Štukelj, J., Svanbäck, S., Agopov, M., Löbmann, K., Strachan, C.J., Rades, T., and Yliruusi, J. (2019a). Direct measurement of amorphous solubility. Anal. Chem. *91*, 7411–7417.

Štukelj, J., Svanbäck, S., Kristl, J., Strachan, C.J., and Yliruusi, J. (2019b). Image-based investigation: biorelevant solubility of α and γ indomethacin. Anal. Chem. *91*, 3997–4003.

Taherimakhsousi, N., MacLeod, B.P., Parlane, F.G.L., Morrissey, T.D., Booker, E.P., Dettelbach, K.E., and Berlinguette, C.P. (2020). Quantifying defects in thin films using machine vision. NPJ Comput. Mater. *6*, 111.

Tan, H., Semin, D., Wacker, M., and Cheetham, J. (2005). An automated screening assay for determination of aqueous equilibrium solubility enabling SPR study during drug lead optimization. JALA *10*, 364–373.

Walker, B., Tamayo, A., Duong, D.T., Dang, X.-D., Kim, C., Granstrom, J., and Nguyen, T.-Q. (2011). A systematic approach to solvent selection based on cohesive energy densities in a Molecular bulk heterojunction system. Adv. Energy Mater. *1*, 221–229.

Wenlock, M.C., Austin, R.P., Potter, T., and Barton, P. (2011). A highly automated assay for determining the aqueous equilibrium solubility of drug discovery compounds. J. Lab. Automation *16*, 276–284.

Zepel, T., Lai, V., Yunker, L.P.E., and Hein, J.E. (2020). Automated liquid-level monitoring and control using computer vision. ChemRxiv. https://doi.org/10.26434/chemrxiv.12798143.v1.

Supplemental information

Automated solubility screening

platform using computer vision

Parisa Shiri, Veronica Lai, Tara Zepel, Daniel Griffin, Jonathan Reifman, Sean Clark, Shad Grunert, Lars P.E. Yunker, Sebastian Steiner, Henry Situ, Fan Yang, Paloma L. Prieto, and Jason E. Hein

Supplemental Information

Contents

Materials and Consumables
Materials

Caffeine was purchased from Sigma Aldrich and was used without further purifications. Acetonitrile (≥99.9%), isopropanol (≥99.9%), acetone (≥99.9%), ethanol (≥99.9%), and methanol (≥99.9%) were purchased from Sigma Aldrich and used without further purifications. Tetrabenazine (TBZ) was synthesized by our group. It is also commercially available at Sigma Aldrich.

Material Consumables on the Platform

Before running the automated system, the deck must be charged with the desired solvents, clean empty HPLC vials with stir bars inside them and the solid of interest inside the Quantos powder dispensing head. BD PrecisionGlide needles (21G, 0.8mm x 25mm) and 2-HPLC vials (Life Science Labs) charged with stir bars (VP Scientific) were used in this workflow. The choice of HPLC vials is due to their convenient small size, which matches the robot's default gripper size and reduces material waste. An inventory of consumables is stored on the system computer. Solvents and solid were refilled by the user upon depletion.

Robotic Hardware
Robotic Deck

The robotic deck consists of an N9 robotic arm (North Robotics, www.northrobotics.com) and additional components needed for the automated solubility workflow secured to the N9 deck. Components were arranged to be easily accessed by the arm while being as compact as possible as shown in Figure S1. The arm controller box (C9, not pictured) includes pneumatic outlets to control the gripper on the arm's head as well as the gripping station on the deck. A gas pressure of 60 psi was supplied to the C9 for this purpose.

For the automated solubility workflow, the arm was used to handle HPLC vials and needles. Vials were moved, uncapped, and recapped using the arm's gripper while a small probe on the arm's head was used to retrieve and discard needles required for liquid dosing. Liquid dosing was performed using a Tecan Cavro syringe pump with 1 mL syringe (off deck). Tubing was run from the pump to the probe to enable on deck dosing from the solvent bank to the reaction vial. Solid dosing was enabled using a Quantos, Mettler Toledo balance, combined with Quantos dosing unit (see Quantos accessories section of the SI for details on modifications). An IKA RCT digital stir plate was used to stir the solutions. and a C920 Logitech webcam was used to capture images for computer vision. All electrical modules (robot, pump, stir plate, balance and dosing unit, and webcam) were connected to the lab computer. Other components on the deck included: needle rack, needle waste bin and beaker for liquid waste, vial tray, vision station, and HPLC cap park station.
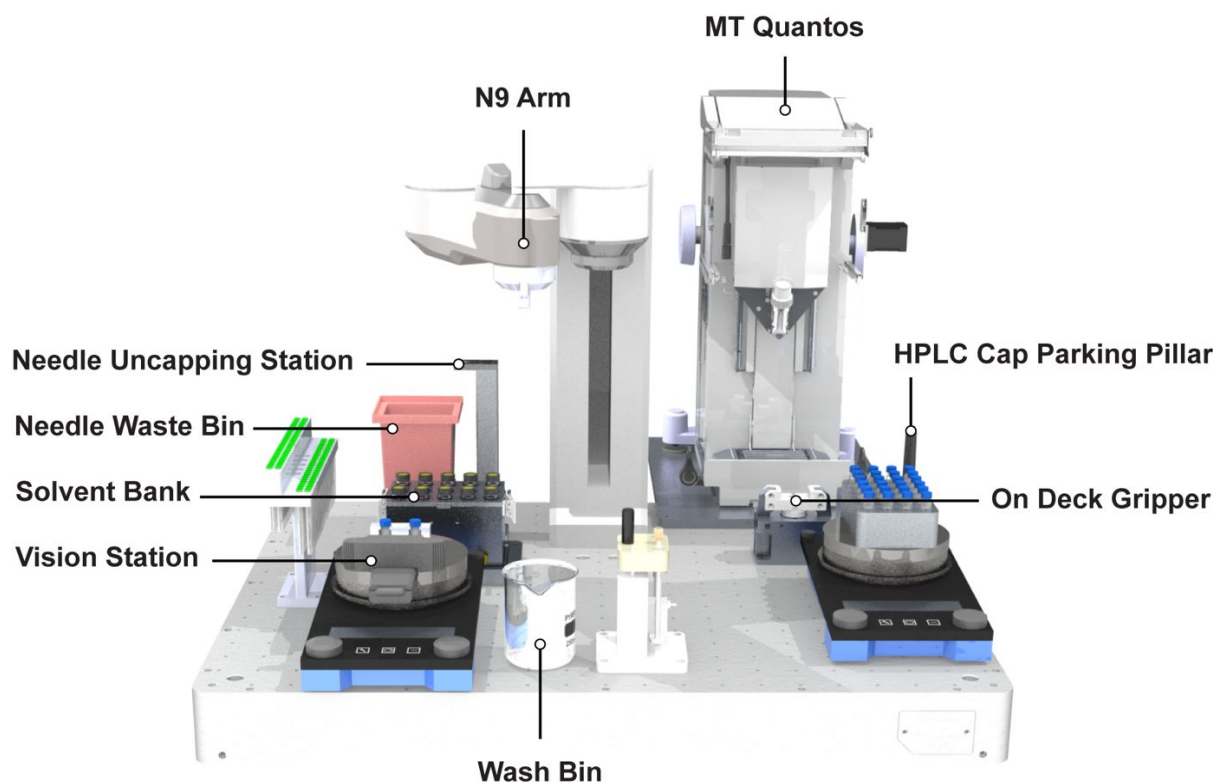
Figure S1. Rendered illustration of the robotic deck with N9 arm and additional components, Related to Figure 1B

System Communication

The modules were connected to the lab computer via serial or USB connections. The C9, stir plate, Arduino controllers and cameras were connected to the computer via USB while communication with Quantos and Kinova arm was over a local network. The Tecan Cavro syringe pump had a serial connection through the C9.

Quantos Accessories

A Quantos Balance XPE205 (220 g capacity, 0.01 mg readability) with powder dosing unit and anti-static kit were purchased from Mettler Toledo and used to enable solid dosing. A variety of dosing heads are available to be used with different solid textures and dosing volumes allow for easy customization. The dosing heads used in the caffeine solubility workflow were BMNP (power characteristics: Ø2.5 mm dosing pin with pushing stirrer, Pinocchio 1 mm nose; max capacity: 8 mL) and LNMP (power characteristics: Ø2.5 mm dosing pin with pushing stirrer, Pinocchio 1 mm nose; max capacity: 12 mL).

Z Stage Control

The Quantos requires manual rotation of a crank to lower the dosing head along the z-axis to meet the opening of the vial. An Arduino (Uno-R3) controlled stepper motor (Nema 17 bipolar, with holding torque of 59 Ncm) was used to automate this process. The motor was mounted on the Quantos side handle, using a machined supporting plate (Figure S2). As the z stage from which the dosing head extends moves up to home position, it hits a limit switch mounted on the inside roof of the Quantos (Figure S3). The number of steps needed to lower the stage to the right height is specified in the code.

PARTS LIST

ITEM	QTY	PART NUMBER
1	1	Quantos Crank Shaft
2	1	Coupler
3	1	Motor Faceplate
4	1	Motor Standoff
5	1	NEMA14
6	3	DIN 912 - M3 x 5
7	2	DIN 912 - M3 x 10
8	2	DIN 912 - M4 x 10
9	2	DIN 912 - M3 x 12

ALL DIMENSIONS IN mm [in] UNLESS OTHERWISE STATED.

GENERAL TOLERANCES:
ONE PLACE DECIMAL ±0.25mm
TWO PLACE DECIMAL ±0.10mm
ANGLES MACHINING ±0.1°

MATERIAL:
SPEC:
FINISH:
WEIGHT: N/A

DRAWN BY: Sebastian Steiner
REVIEWED BY:
APPROVED BY:
DESCRIPTION:
Stepper motor assembly
MT Quantos

DATE: 2019-10-23
SIZE: A
SCALE: 1 : 1
SHEET: 1 / 1

© Hein Lab 2019

Figure S2. Exploded view of stepper motor assembly. Related to Figure 1A (solid dosing unit)

PARTS LIST

ITEM	QTY	PART NUMBER
1	1	Mettler Toledo Quantos
2	1	Switch holder base plate
3	1	Switch holder middle plate
4	1	Switch holder top plate
5	1	Limit Switch
6	2	DIN 912 - M2 x 10
7	2	DIN 912 - M4 x 12
8	2	DIN 7991 - M3x8
9	2	DIN 912 - M3 x 8

ALL DIMENSIONS IN mm [in] UNLESS OTHERWISE STATED.

GENERAL TOLERANCES:
ONE PLACE DECIMAL ±0.25mm
TWO PLACE DECIMAL ±0.10mm
ANGLES MACHINING ±0.1°

MATERIAL:
SPEC:
FINISH:
WEIGHT: N/A

DRAWN BY: Sebastian Steiner
REVIEWED BY:
APPROVED BY:
DESCRIPTION:
Limit Switch Assembly
MT Quantos

DATE: 2019-10-23
SIZE: A
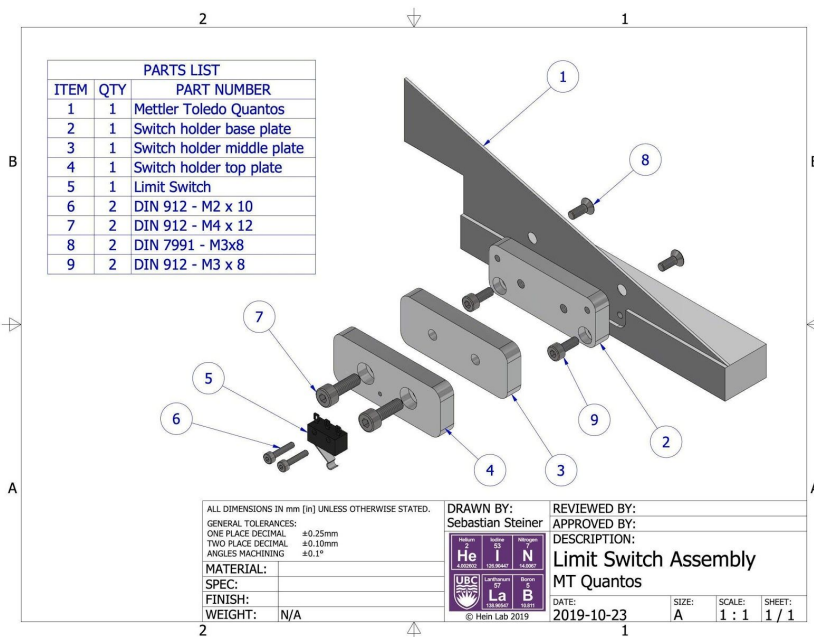SCALE: 1 : 1
SHEET: 1 / 1

© Hein Lab 2019

Figure S3. Exploded view of the switch assembly, Related to Figure 1A (solid dosing unit)

Mounting Plates and Vial Holder

The Quantos is held in place using two auxiliary aluminium plates and a supporting back foot, which are screwed to the deck. A 3D-printed HPLC vial holder was designed (Figure S4) and placed inside the Quantos to ensure vial stability during weighing and dosing processes.
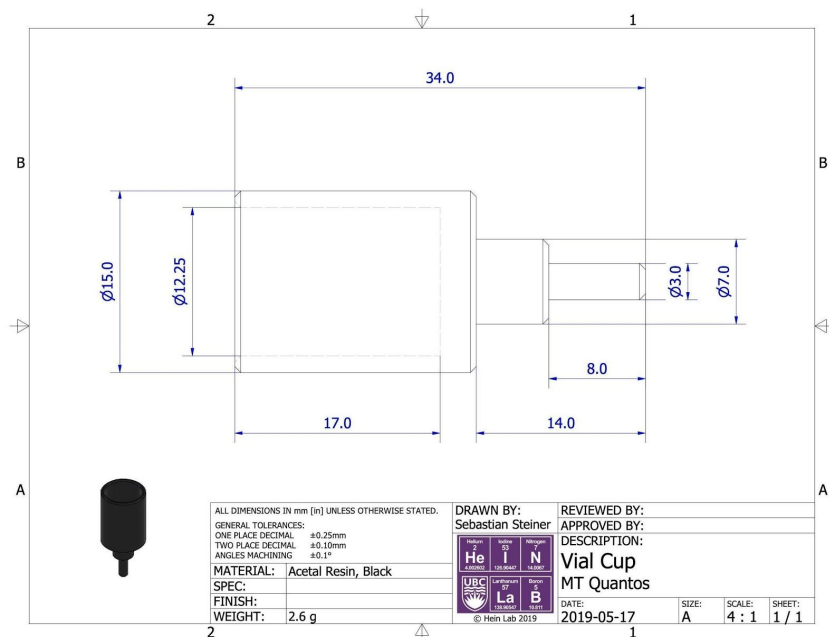

Figure S4. Quantos vial holder assembly, Related to Figure 1A (solid dosing unit)

Uncapping

Secure uncapping and recapping of vials were facilitated using the capabilities of the N9 arm and in combination with a custom designed 3D printed parking pillar. Prior to solid dosing, the vial was moved to the static gripper on deck. The N9 arm was then used to twist the vial caps by performing a simultaneous upward and rotational movement. Caps were temporarily parked on 3D printed pillar (Figure S5) in order to free the arm's gripper to handle vials as the workflow continued. Vials were recapped prior to turbidity monitoring to prevent evaporation of volatile solvents. Initial difficulty with proper cap sealing led to the implementation of a torque feedback reading from the C9 to ensure that each vial was properly capped. The torque value associated with proper capping was identified and used as a threshold after the recapping step: if the current torque reading was smaller than the threshold, the arm's gripper tightened the cap by 1 degree increments until the threshold was reached.
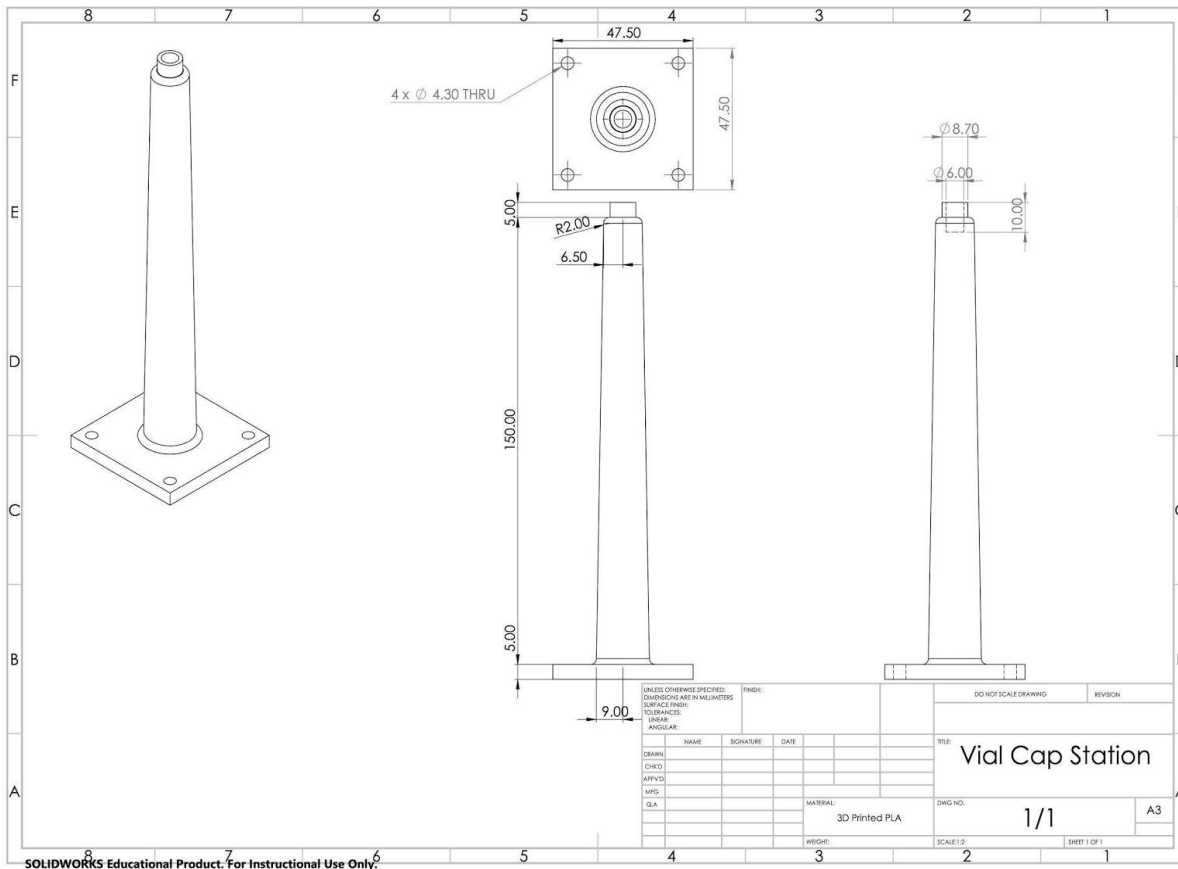
Figure S5. HPLC cap parking pillar assembly, Related to Figure 1B

Vision Station

The vision station is composed of the stir plate, webcam and a custom 3D printed vial holder, spray painted matte black (Figure S6). The holder is secured to the plate with tape and designed to enable simultaneous stirring, imaging, and solvent addition. An open front allows the camera to see the contents of the vial during stirring while a collar acts as a stopper to keep the capped vials in place when piercing through the septa with a needle to dose liquids. The holder was painted matte black after printing to minimize glare on the vials, which interfered with turbidity measurements output by the computer vision algorithm.
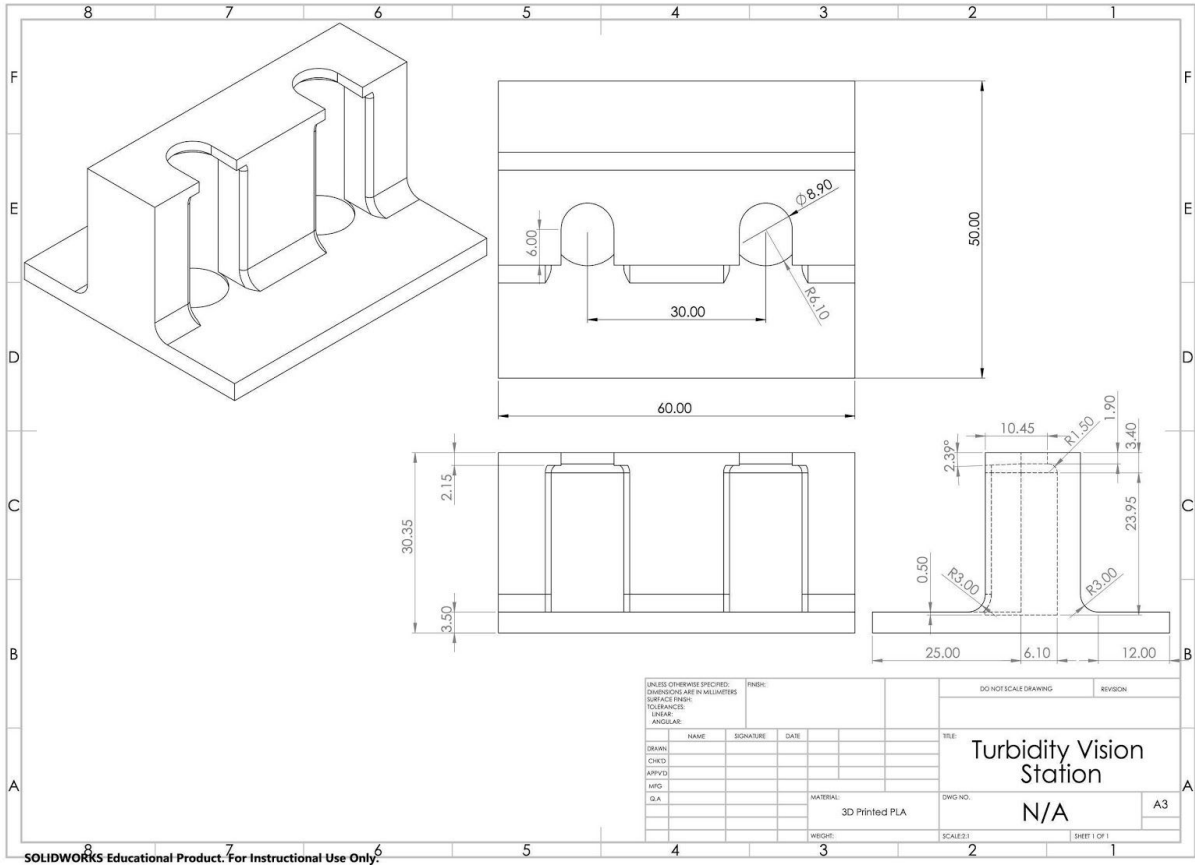
Figure S6. Vision station assembly, Related to Figure 5

Remote Control and Development

Development and testing were performed remotely following initial placement of the hardware and recording of reach locations. The Chrome remote desktop application was used to access the system computer and input initial settings while a surveillance camera positioned above the deck provided means for observation during remote operation.

The platform also made use of Slack, an online messaging platform. The Slack Developer Kit for Python was used to configure a custom Slack app to send updates and provide real-time monitoring and control. Table S1 details the programmed commands that can be sent via Slack on a pre-specified channel to access and control the platform during an active run. Responses are sent as messages with the requested content and posted to the same channel. A final report (Figure S7) is generated and automatically sent at the end of each run.

Table S1. Slack commands for live control and manipulation of the system, Related to Robotic Methods (Step 4)

|	
vial image	Send the current image from camera aimed at vials in the vision station
deck image	Send the current image from camera aimed at the deck
get needle	Get and uncap a needle
uncap needle	Uncap a needle already on the probe
dump needle	Remove a needle
main resume	If the run paused at a specific point, use this to resume the run
graph	Send a graph of turbidity vs. time
add solvent	Add a step addition volume of solvent into a vial in the vision station
clean up vial	Clean up the current vial
start next vial	Start the next experiment, clean up the current vial if required
don't start next vial	Don't start the next experiment
roi	Send the current image from camera with the region of interest drawn on the image aimed at the vision station
change stir rate [number]	Change the stir rate to the specified number
set dissolved reference [number]	Change the fully dissolved turbidity reference to the specified number
turbidity video	Send a video from all the images used to make turbidity measurements from the camera aimed at the vision station for the current run
use next solvent	For the next run, use the next solvent in the sequence to test
pause solvent addition	Pause solvent addition
resume solvent addition	Resume solvent addition if paused
pause monitoring	Pause turbidity monitoring
resume monitoring	Resume turbidity monitoring if paused
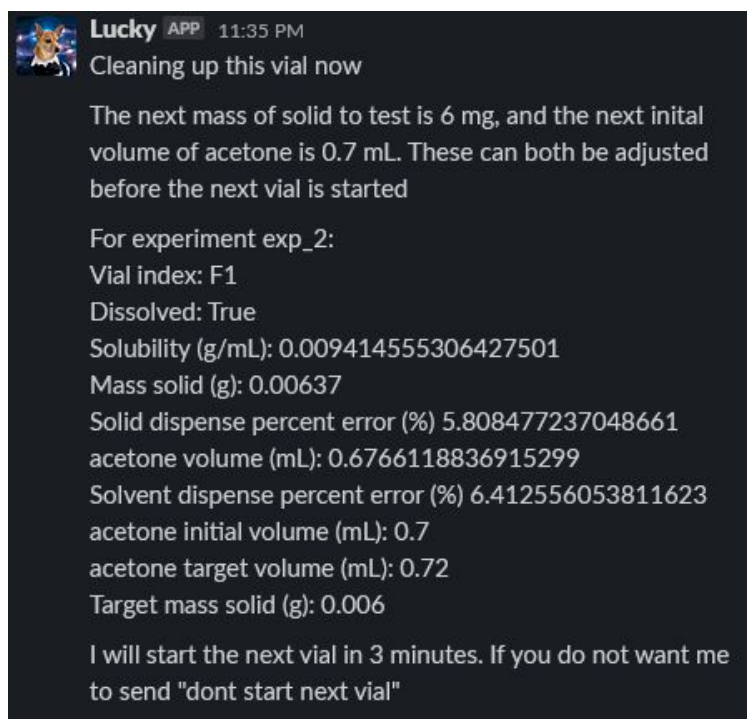
Figure S7. Sample final report generated and sent through Slack, Related to Robotic Methods (Step 4)

Supplementary Computer Vision Methods
Visual Needle Detection

Computer vision was used to confirm that needle components were retrieved and removed as expected. Failure to do so could cause errors in the experimental data or result in broken glassware. In the case of a failed removal or retrieval the researcher is notified via Slack.

Confirmation of proper needle retrieval and removal relies on a script that uses the colour matching and ROI modules in the HeinSight Python package. Following a programmed needle retrieval, the N9 moves to a specific position on the deck where the webcam takes a photo of the area below the arm's probe. The colours in a pre-selected ROI in this photo are compared to a reference photo in which the needle was picked up successfully (Figure S8). If the average colour within the region where the needle is expected to be is similar to the colour in the reference photo, it is concluded that the needle is on the N9 probe. A similar process checks for needle removal. Following a programmed removal, the N9 moves to the same deck position where a new photo is taken. The colours in the specified ROI are compared to a reference photo in which the needle was successfully removed. In either case, if the needle was not successfully retrieved or removed, the automated workflow is paused, and a message is sent via Slack to the researcher who can try to correct the situation remotely by directing the N9 to repeat the retrieval or removal actions.

The visual check only needs to be set up once before it can be used multiple times. For set up, the N9 arm picks up a needle on the probe and brings it to the check location to visually record three different needle states: capped (needle is encased in protective covering), uncapped (protective covering removed), and absent (needle has been removed from the probe). The researcher is presented with an image where the needle is on the probe and is prompted to interactively select the region in the image that will be used for the needle check. A file with all the parameters for needle detection is then saved and can be loaded for future use. The results of the needle detection on the three collected images are

displayed to the user and if the results do not match with the actual state, the researcher might have to adjust the needle detection parameters, lighting conditions, or the position where webcam captures photos to be used in error detection.
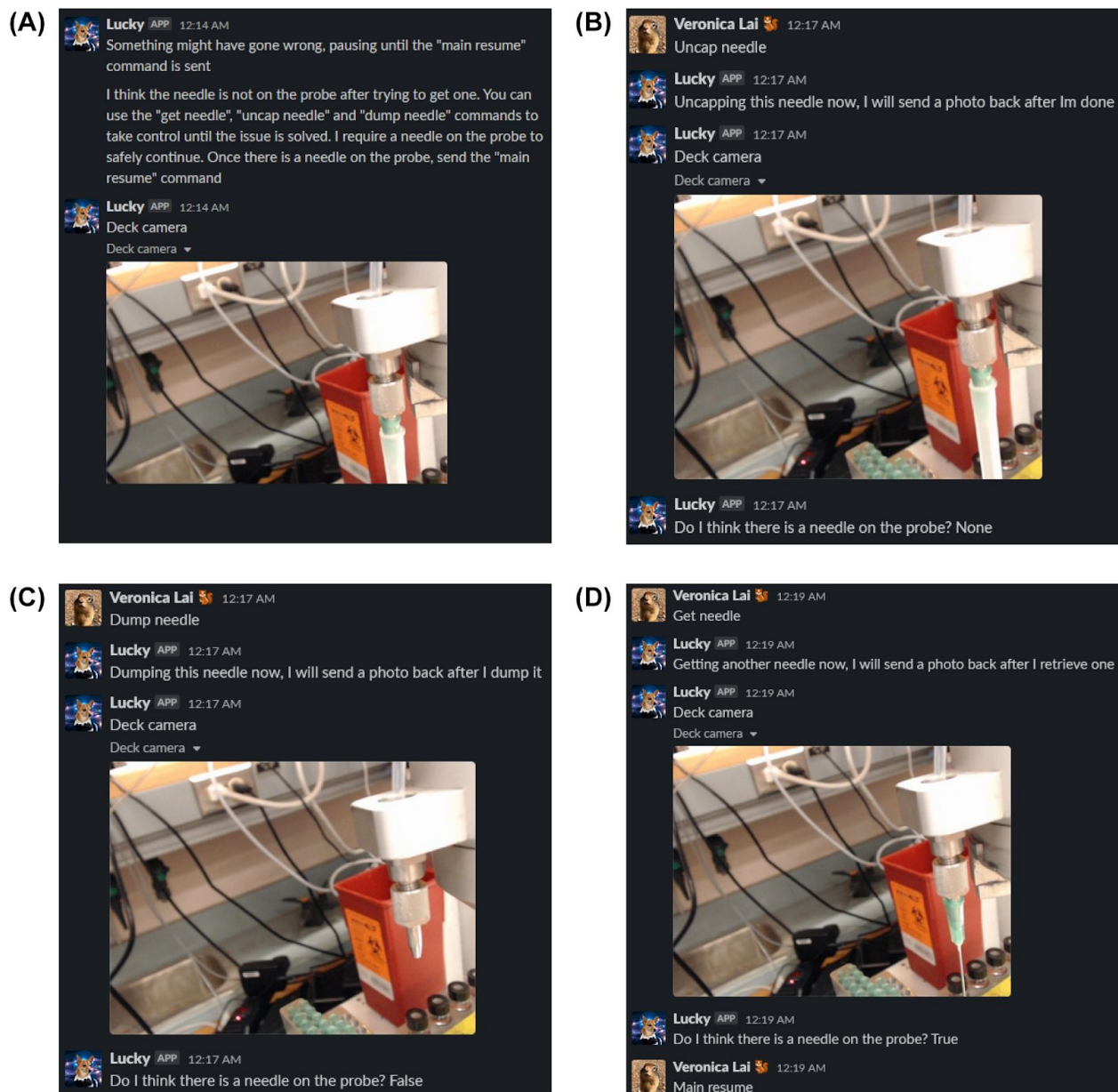
Figure S8. Slack messages related to vision checks of needle state, Related to Robotic Methods (Step 2)
(A), after unsuccessfully retrieving and uncapping a needle, a message was sent by the Slack app detailing the issue and prompting the researcher to take control to remedy the issue. (B), a command to uncap the protective covering was sent, but it looks like there is an issue most likely because the covering was on too tight. (C), the command to remove the needle is sent and was executed successfully. (D), the command to retrieve and uncap a needle was sent and was executed successfully, and the command to resume the experiment was sent.

Turbidity Monitoring Dissolution Point

When the algorithm monitors turbidity, several steps are executed to determine whether a sample is fully dissolved. Samples are considered dissolved if the turbidity has stabilized at the reference value or if the turbidity measurements over the five most recent minutes are all below the reference value. To account for cases where large solid particles remain but do not contribute to the solubility measurement, the stir rate is increased to strongly agitate and break down any remaining chunks. After five minutes of strong stirring the stir rate is reduced back to the normal rate and the turbidity is monitored for another five minutes. After this second round of monitoring, the dissolution check is repeated. If the sample is considered dissolved this second time the workflow will proceed to the clean-up stage. If the sample is determined not to be dissolved, turbidity monitoring is resumed. In this case, the next time the sample looks dissolved the increased stir rate and a second dissolution check is performed again.

Computer Vision Challenges for Turbidity

There are limitations to our visual proxy measurement of turbidity. As the algorithm uses brightness as a proxy for turbidity, it works best when there is high contrast between the solution being measured and the visual backdrop. For the caffeine implementation, the solution appears bright (white) when turbid and dark (clear) when dissolved because the colourless solution is placed in front of the black background of the vial holder. This contrast enables the algorithm to assign distinct brightness values to the turbid and clear solutions. The TBZ implementation was meant to challenge the computer vision algorithm. While solid TBZ has a yellowish tint, the solution is still brighter when turbid. Thus, the algorithm was able to distinguish between the turbid and dissolved solution when placed against the dark background. Other challenges related to computer vision arose from visual artifacts that may interfere with the algorithm's ability to interpret the visual properties of the solution within the selected region of interest. Initial experiments with TBZ and acetone produced inconsistent solubility values because of the tendency for solid particles to cling to the inside of the vial walls when not properly cleaned. The algorithm thus read the solution as brighter than it actually was. Future work is already underway to account for solid clumping.

Abrupt changes in the visual environment can also affect the turbidity. Because the algorithm is programmed to measure brightness in a fixed region of the image, slight changes in camera angle or vial position can result in an inconsistent measurement of solution turbidity. For example, we observed that the stir bar moving in and out of the region of interest resulted in noisy turbidity measurements. Light glare off the glass and the general lighting environment will also affect the turbidity measurement. We therefore tried to keep the visual environment as constant as possible. An ROI was selected away from the stir bar, lab lights were kept on overnight, and the platform was placed away from the window to reduce variance due to fluctuations in natural lighting. It should be noted that fluctuations in lighting are a challenge for any computer vision method and are not specific to the proxy measurement.

Ambient Light Study

The large number of windows in our laboratory lead to significant fluctuations in ambient light. To investigate the degree to which ambient light affects the turbidity value output by the algorithm, we used the system to monitor the turbidity of water at different time intervals throughout the day (Figure S9). Fluctuations in sunlight and researchers moving around the benchtop set-up during daylight hours result in a far more inconsistent lighting environment than at night.

Figure S9 shows data gathered during each run along with an image of the ROI and normalization region selections. As expected, relatively turbidity varied less during the evening (top three graphs) than during the day (bottom graph). The increased variance in inconsistent lighting environments is a result of the turbidity algorithm's reliance on brightness as a proxy for turbidity. Measurements are thus most reliable when a consistent lighting environment can be ensured.

The difference in turbidity values between each run can be explained by the different ROI and normalization region selections for each run. Because the determination of when a solution is dissolved is based on monitoring turbidity against a reference for each individual run, the turbidity inconsistency between runs does not introduce error.
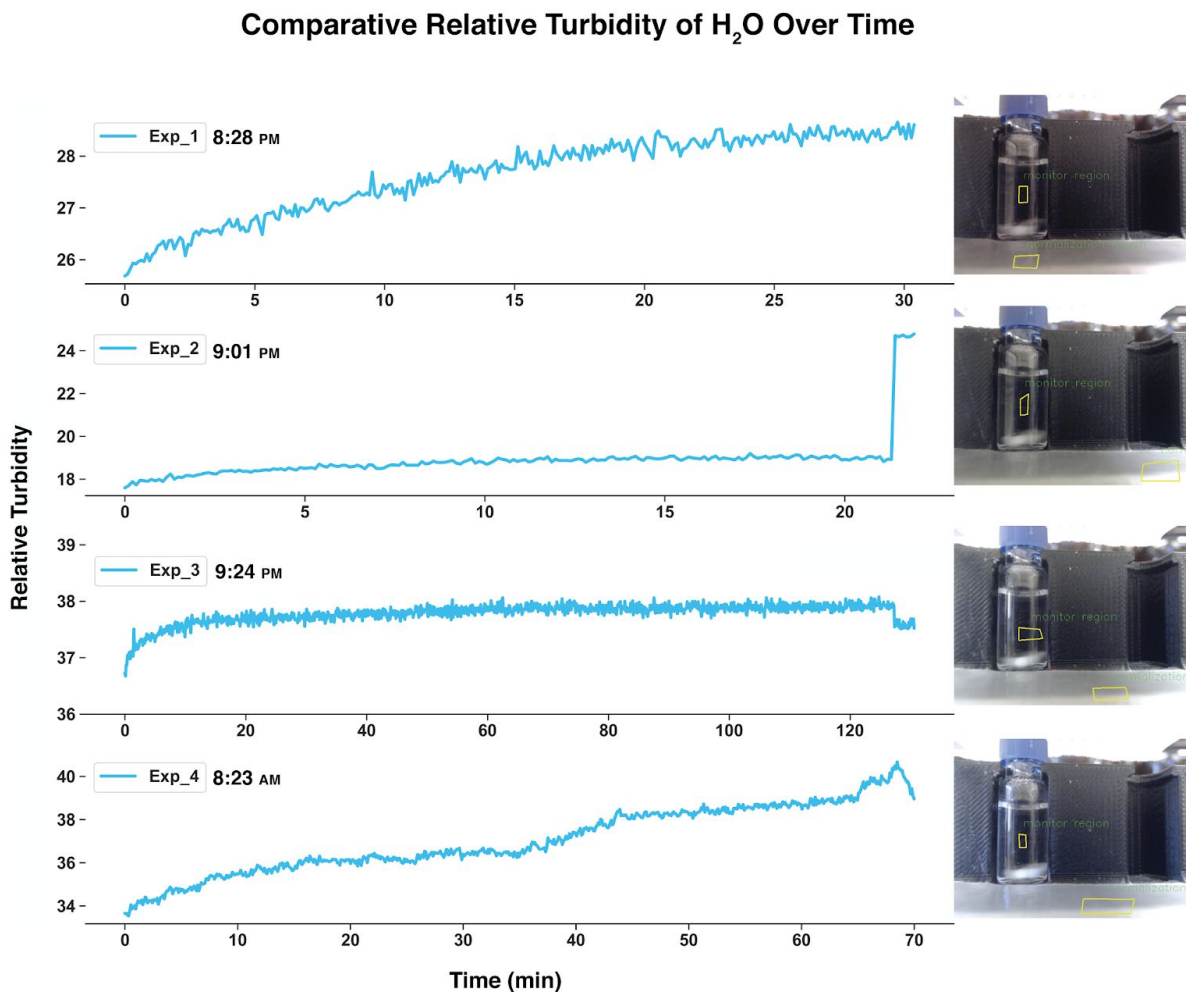

Comparative Relative Turbidity of H$_2$O Over Time

Figure S9. Relative turbidity of H$_2$O at different daylight intervals, Related to Figure 6

For each graph a corresponding image of the vision station and with the ROI and normalization region annotated on the image are presented. The top three graphs correspond to evening runs. The bottom graph corresponds to a run conducted during the day when fluctuations in sunlight caused fluctuations in ambient light in the room. In the second top graph, Exp_2, the sharp increase at the end is due to the bright lock screen wallpaper of the computer when it was woken from sleep and used to stop the experiment; the computer directly faced the front of the vision station. For the third graph, Exp_3, there is a slight decrease at the end, which is likely due to the lock screen wallpaper.

Duplication on Kinova Platform

Liquid Handling Setup (Sampleomatic)

Duplication of the workflow for use with the Kinova arm required a different liquid dosing system due to positioning of the arm and the absence of a needle probe. Figure S10 shows a diagram of the modified liquid dosing module as implemented. In this set-up, a number of solvent bottles are connected to a selection VICI valve, which is connected to a Tecan Cavro pump. Single-use needles are replaced by a

custom sampler called the "sampleomatic" (Fig S11). A Gilson probe (162 x 1.2 x 0.4 mm Beveled 0.7 Tip) is attached to a handle and mounted on a rigid base with a hole and draining outlet to allow for flushing of the line and needle extension. The probe is driven by an Arduino controlled motor (external linear actuator, Nema 11 - LSA281S10-A-THCA-152). The handle was designed and 3D printed such that the Robotiq gripper on Kinova could pick up and handle it securely.

10-port Selection Valve

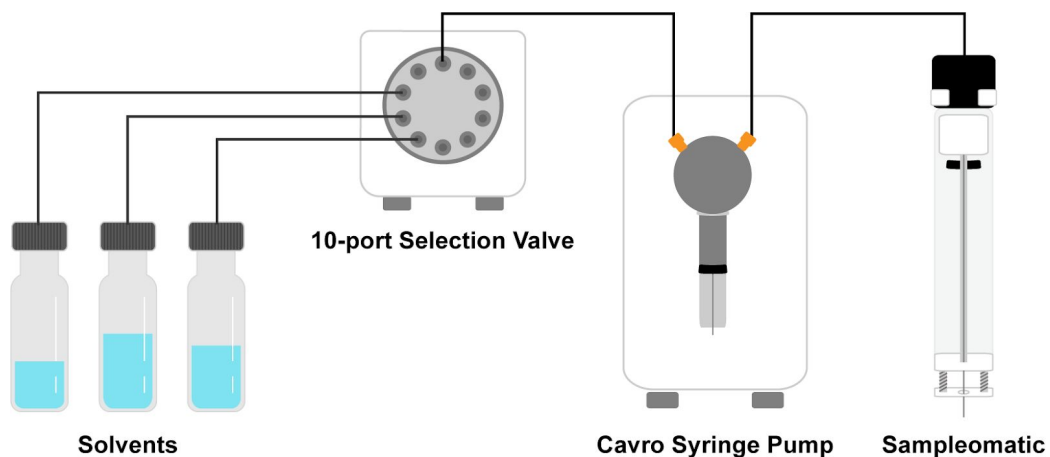**Solvents**   **Cavro Syringe Pump**   **Sampleomatic**

Figure S10. Diagram of liquid handling system used by the Kinova platform, Related to Figure 7
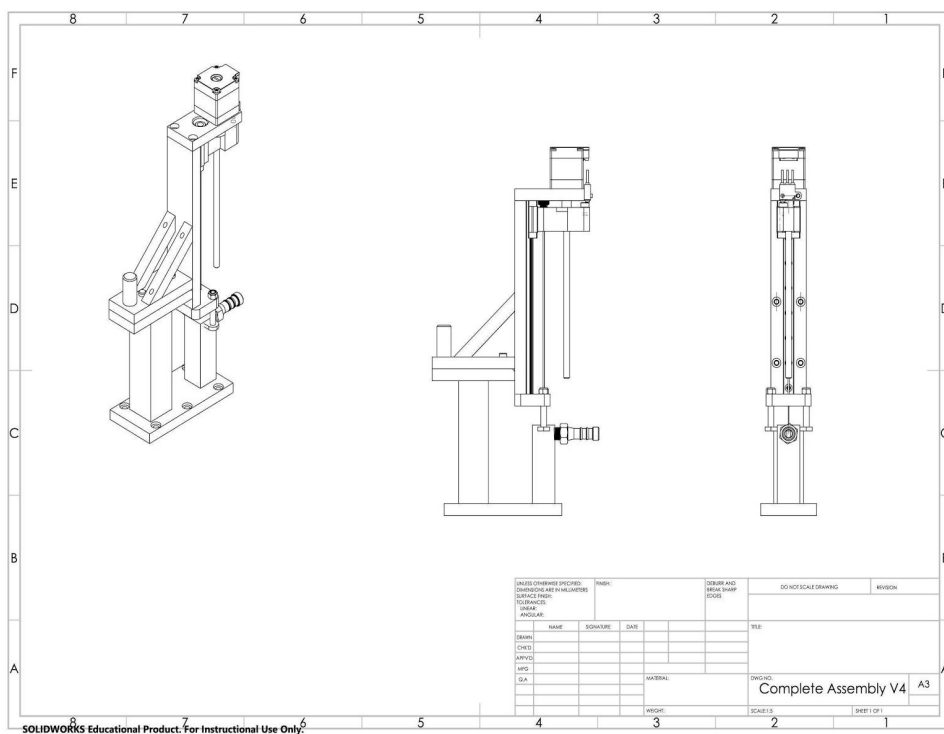

Figure S11. Sampleomatic assembly (top and base), Related to Figure 7

Uncapping Vials with Kinova

HPLC vial uncapping on the N9 platform was facilitated by an on-deck vial gripper. In the Kinova setup, O-ring press fit vial locations were used to grip the vial while the gripper on the arm performed the vertical twist motion for uncapping procedure. Due to the arm speed and limitation of rotating only 90 degree increments at a time without changing direction, the uncapping was broken down into a few movements, rotating about 90 degrees at a time until capping and uncapping was achieved. A screw top was used as a parking station for the caps.

Manual Data Collection Process

Solubility values for comparison were obtained via manual titration and slurry methods. A Mettler Toledo balance was used to measure solids. Liquid volumes < 1 mL were measured and dosed using pipettes while quantitative volumetric flasks were used for all other volumes. An Agilent 1290 UHPLC with an Acquity UPLC BEH C18 $1.7 m$, 2.1 x 50 mm column and two phases of water + 0.1% trifluoroacetic acid (TFA) and acetonitrile were used to analyse the solution for the slurry method. The flow rate was 0.5 ml/min. Two standards were prepared with the concentration of 0.2 m/ml caffeine in HPLC grade acetonitrile. The solutions were sampled after shaking by the HPLC autosampler. For the slurry method process, ~50 mg of caffeine was added to HPLC vials, and 1ml of each solvent in the screen was added to them and shook for 24 hours at 25 °C. Then ~1 mL of each vial was transferred to filtered disposable centrifuge tubes and centrifuged for about 1 min at 7 g. The filtered solids were discarded and 0.1 mL of each system was added to a 10 mL volumetric flask using a manual pipette with a fresh tip. Each system was diluted by x100 factor and the calibrated UPHCL was used to determine the solubility of caffeine in each solvent.

User Documentation

All scripts and custom packages used are available for download at:
https://gitlab.com/heingroup/automated_solubility_h1

Running the workflow requires no prior knowledge of the individual modules and involves the same steps regardless of the arm in use (N9 or Kinova). All files referenced can be found in the referenced gitlab repository. Additional instructions related to code manipulation can be found in comments within individual files.

1) Stock the platform with the appropriate consumables including needles, clean HPLC vials (pre-loaded with stir bars), and desired solvents. Add the desired solid to the correct Quantos dosing head based on grain size. Insert the head filled with solid into the Quantos and follow the prompts to input the details of the powder. Ensure that the sharp bin and solvent waste container on deck are clean.
2) Set the desired paths for saving data:
    a) `n9/experiments/main_solubility.py` - create_experiment_folder()
    b) `n9/configuration/deck.py` - position_record()
    c) `n9/configuration/deck.py` - lines 66, 87, 116, 132 - 135, and 138.
3) If Slack integration is desired:
    a) Ensure access to a Slack channel and a Slack app to send messages to the channel.
    b) Then open and edit the file fields in the
       `n9/experiments/solubility_vision_slack_manager_info.py`:

i)   `bot_token`: Slack app bot user access token, must start with "xoxb"

ii)   `bot_name`: name of the Slack app

iii)   `channel_name`: name of the Slack channel the app is in to send commands and receive updates in

4) Open the stock_info.csv and `vial_info.csv` and edit to match experimental materials. Update the `stock_info.csv` with name, density, location and initial volume of the stock solvents. In `vial_info.csv`, set the last column to 'False' (these values will automatically update to 'True' as each vial is used by the system).

5) Open the `main n9/experiments/main_solubility.py` script.

   a) Input initial values required by the system (lines 1360 and 1375) including stir rate, list of solvents for screening, initial volume of solid, volume of each step addition, and initial volume.*

      * The logic of the code assumes an initial solid mass of 6 mg. Initial solvent volume should be set to 0.5 ml or less to allow enough room for step addition of solvent and monitoring.

6) Run the script.

7) The first vial will be moved to the vision station, dosed with an initial amount of solvent and stirring will begin. A window will pop up prompting the user to set the normalization region and region of interest (ROI).

   a) Set the normalization region by clicking on at least three points that outline an area in the image that will remain constant (no movement or fluctuations in lighting) and is not inside the reaction vial. Hit the space key.

   b) A prompt to set the ROI for turbidity monitoring will pop up. Set this region using the same three or more point and click method. Ensure that the location of the ROI is an area where liquid will be present and does not overlap with the stir bar or any hard light due to vial reflection. The black background should be clearly visible to ensure optimal algorithm performance. I This region should be chosen to fit a location where the solution will be present.

8) After this initial set-up, the run will continue until completion without interruption unless otherwise prompted or consumables need to be refilled. Solubility data will be automatically saved to the specified folder and the user will be notified with regular updates via Slack (if enabled). Please refer to the Robotic Methods section in the main text for detailed information about how the details on the logic and how workflow proceeds.

SUPPLEMENTARY DATA

Table S2. Overall data from the runs with the N9 platform, Related to Table 1

Solvent	Mass solid (g)	Volume solvent (mL)	Solubility (g/mL)
acetone	0.00823	0.82174463	0.01001527
acetone	0.00851	0.82667509	0.01029424
acetone	0.00814	0.80240202	0.01014454
acetone	0.00805	0.84791403	0.00949388
water	0.00729	0.4279123	0.01703669
water	0.00899	0.4892356	0.01837694
water	0.00835	0.444	0.01880631
water	0.00860	0.4609	0.01865915
ethanol	0.00471	0.85361217	0.00551773
ethanol	0.00453	0.84334601	0.00537146
ethanol	0.00455	0.87084918	0.00522479
ethanol	0.00429	0.79632446	0.00538725
methanol	0.0063	0.71163085	0.0088529
methanol	0.0069	0.77079646	0.00895178
methanol	0.00616	0.79620733	0.00773668
methanol	0.00602	0.76207332	0.0078995
acetonitrile	0.00921	0.51272265	0.01796293
acetonitrile	0.02157	0.52697201	0.0215761
acetonitrile	0.02034	0.110005	0.01849
acetonitrile	0.0936	0.49987277	0.01872476

Table S3. Overall data from the runs with the N9 and Kinova platform, Related to Table 2

Platform	Solute	Solvent	Mass solid (g)	Volume solvent (mL)	Solubility (g/mL)
N9	TBZ	acetone	0.04983	0.56238520	0.088604749
N9	TBZ	acetone	0.0505	0.57447704	0.0879060
N9	TBZ	acetone	0.04984	0.56714285	0.08787909
N9	TBZ	ethanol	0.00795	0.47681	0.01667345
N9	TBZ	ethanol	0.00823	0.51891	0.01586017
N9	TBZ	ethanol	0.00828	0.50601	0.01636339
N9	TBZ	acetonitrile	0.03248	0.49475827	0.06564822
N9	TBZ	acetonitrile	0.04603	0.66620865	0.06909247
N9	TBZ	acetonitrile	0.04619	0.67235369	0.06869896
N9	TBZ	methanol	0.02237	0.90982	0.02458721
N9	TBZ	methanol	0.0223	0.894	0.02494407
N9	TBZ	methanol	0.02226	0.87004	0.02558509
Kinova	TBZ	acetone	0.06054	0.6858407	0.0882712
Kinova	TBZ	acetone	0.0608	0.67012642	0.0907291
Kinova	TBZ	acetone	0.0603	0.68582161	0.08792378
Kinova	TBZ	ethanol	0.01504	0.95145385	0.015807387
Kinova	TBZ	ethanol	0.01001	0.56532237	0.017706711
Kinova	TBZ	ethanol	0.01512	1.00558935	0.015035958
Kinova	TBZ	acetonitrile	0.05031	0.7376972	0.068198713
Kinova	TBZ	acetonitrile	0.05661	0.73260814	0.07727186
Kinova	TBZ	acetonitrile	0.03801	0.65207379	0.058290948
Kinova	TBZ	methanol	0.01604	0.64396965	0.024908006
Kinova	TBZ	methanol	0.01553	0.63546144	0.02443893
Kinova	TBZ	methanol	0.0159	0.65687737	0.024205431
Kinova	caffeine	acetonitrile	0.02122	0.99877862	0.02124594
Kinova	caffeine	acetonitrile	0.02218	1.03632315	0.02140259
Kinova	caffeine	acetonitrile	0.01534	0.64445292	0.02380313
Kinova	caffeine	ethanol	0.00411	0.92262357	0.00445468
Kinova	caffeine	ethanol	0.00314	0.80613434	0.00389513